Physicochemical Characterization of Subporphyrazines—Lower Subphthalocyanine Homologues

ARTICLE *in* CHEMSUSCHEM · APRIL 2009

Impact Factor: 7.66 · DOI: 10.1002/cssc.200800182 · Source: PubMed

6 AUTHORS, INCLUDING:

Esmeralda Caballero
Universidad Autónoma de Madrid
21 PUBLICATIONS **187** CITATIONS

CHEMSUSCHEM

DOI: 10.1002/cssc.200800182

Physicochemical Characterization of Subporphyrazines—Lower Subphthalocyanine Homologues

G. M. Aminur Rahman,[a] Daniela Lüders,[a] M. Salomé Rodríguez-Morgade,[b] Esmeralda Caballero,[b] Tomás Torres,*[b] and Dirk M. Guldi*[a]

Physicochemical characterization of boron(III) subporphyrazines (SubPzs)—lower subphthalocyanine (SubPc) homologues—has been carried out for the first time. The SubPz macrocycle can act both as an oxidizing and a reducing entity, giving rise to stable radical anion or radical cation species, respectively. SubPzs are luminescent and exhibit fluorescence quantum yields that are in the range known for SubPcs. The peripheral substitution plays a dramatic role with respect to the luminescence properties. Moreover, as with SubPcs, deactivation of the singlet excited state of the SubPzs by intersystem crossing affords long-lived triplet excited states, which are amenable to being used as singlet-oxygen generators. Subporphyrazines are also promising electro- and photoactive materials for molecular photovoltaics.

Introduction

Organic solar cells based on phthalocyanines[1] (Pcs) are a promising way towards efficient photovoltaic (PV) systems. The development of novel dyes based on Pc analogues is an important goal to be pursued. The singular structural features of subphthalocyanines (SubPcs, **1**; Figure 1)[2,3] are directly related

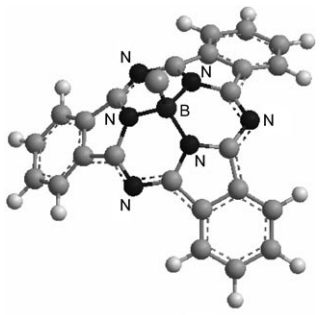

1

Figure 1. Molecular structure of boron(III) subphthalocyanine.

to their pre-eminence among other azaporphyrin analogues. Thus, these ring-contracted phthalocyanine congeners gather much attention because they are 14 π-electron, cone-shaped aromatic surfaces that show little or no aggregation in solution, and this feature provides them with intrinsic chemical and physical properties.[2] Also, the C_{3v} symmetry of the SubPc core endows these macrocycles with octupolar character, while the boron(III) ion coordinated by the macrocyclic ligand is responsible for charge transfer within the π surface of the macrocycle. These two features taken together, and combined with appropriate functionalization on the axial and at the peripheral positions, have successfully been employed to obtain efficient second-harmonic generators.[4]

Boron(III) subphthalocyanines show intense fluorescence,[5] with average quantum yields of $\Phi_F \approx 0.25$ (about half of that observed for highly fluorescent phthalocyanines such as AlPcCl) and with emission spectra that are mirror images of the absorption bands. Noticeably, deactivation channels such as intersystem crossing are more efficient for SubPcs than for Pcs and, consequently, boron(III) subphthalocyanines present excited singlet states with a lifetime (τ_S) of about 3 ns, which is about half the value observed for phthalocyanines. This results in larger quantum yields and a longer-lived (100 μs) triplet state for SubPcs.[2] Therefore, the SubPc molecule constitutes a superb photosensitizer, producing singlet oxygen with a high efficiency.

With the goal of understanding the basic processes of photoinduced electron transfer in photoactive SubPc-containing ensembles, different electroactive moities have been coupled to these macrocycles in order to construct multifunctional donor–acceptor hybrids for application in molecular photovoltaics.[6] Thus, SubPcs were shown to be excellent electron-donor units when linked in their axial position to fullerene (C_{60}). Moreover, a boron(III) subphthalocyanine moiety may act as the electron-accepting counterpart when linked to strong donating molecules such as ferrocene (Fc) or triphenylamine.

[a] *Dr. G. M. A. Rahman, D. Lüders, Prof. Dr. D. M. Guldi*
Department of Chemistry and Pharmacy
& Interdisciplinary Center for Molecular Materials
Friedrich-Alexander-Universität Erlangen-Nürnberg
Egerlandstrasse 3, 91058 Erlangen (Germany)
Fax: (+49) 9131-8528307
E-mail: dirk.guldi@chemie.uni-erlangen.de

[b] *Dr. M. S. Rodríguez-Morgade, Dr. E. Caballero, Prof. T. Torres*
Departamento de Química Orgánica (C-I)
Universidad Autónoma de Madrid
Cantoblanco, 28049 Madrid (Spain)
Fax: (+34) 914-973-966
E-mail: tomas.torres@uam.es

In addition, the energy level of the charge-transfer state may be tuned by peripheral functionalization of the SubPc unit with substituents of different electronic character.

Examples of the use of boron(III) subphthalocyanines for the fabrication of PV devices have also been reported.[7] Thus, subphthalocyanine films in combination with C_{60} have been studied in a planar bilayer donor–acceptor heterojunction, and a power efficiency of 3% under 1 sun was measured.

We have designed and prepared a variety of SubPc derivatives that exhibit specific properties for their application in different fields. For example, the subphthalocyanine periphery has been functionalized with groups of different nature to assemble subphthalocyanine-based π-extended oligomers,[8] or metallosupramolecular cages.[9] In other cases, materials showing mesomorphic behavior,[10] sensing abilities,[11] or LED applications, among others, were pursued. Very recently, other groups have reported related systems: the subporphyrins.[12,13] Furthermore, diverse functions have been introduced on the axial position to modulate the properties of these compounds and obtain tailored materials,[6] as well as to assemble subphthalocyanine μ-oxo dimers,[14] "back-to-back" B-B-linked subphthalocyanine dimers,[15] and one-dimensional supramolecular architectures in the crystalline state.[16]

We recently described the preparation, structural characterization, and mesomorphic behavior of a new family of tripyrrolic macrocycles by formal replacement of the three isoindole subunits in a SubPc by three pyrrole rings.[17] The resulting subporphyrazines (SubPzs, **2**; Figure 2) retained the conical shape

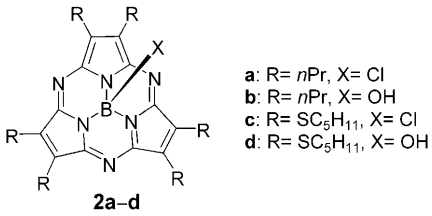

Figure 2. The boron(III) subporphyrazines studied herein.

and aromatic nature of subphthalocyanines, while their absorption profiles, reactivity, and supramolecular organization could be tailored.[16,17] The latter issue is very important in solar cells, as it is essential to have control over the nanometer-scale two-dimensional organization of donor–acceptor mixture-containing dyes for efficient charge flow within a bulk heterojunction. In this context, both subphthalocyanines and subporphyrazines have shown a one-dimensional columnar organization in the solid state.[16]

Notably, peripheral substitution provided a powerful synthetic tool with which to efficiently modulate the optical properties of these macrocycles, because in these systems the substituents are directly attached at the β-positions of the pyrrole moieties, and as for porphyrazines the coupling between the peripheral groups and the aromatic azaporphyrinic core is considerably enhanced.[18] Here, we now report photophysical studies on these compounds and explore the effects of the substituents on the excited states.

Results and Discussion

Subporphyrazines **2a–d** were prepared as previously described by treatment of the corresponding maleonitriles with boron trichloride in xylene at reflux temperature.[17] Under these conditions, the axially substituted chloro derivatives **2a** (22%) and **2c** (8%) were isolated. Further hydrolysis afforded the corresponding boron(III) hydroxysubporphyrazines **2b** and **2d** (8 and 5%, respectively, from the corresponding maleonitriles).[17]

The UV/Vis spectra of subporphyrazines **2a–d** exhibit Soret and Q-bands at such energies that they reflect the lack of the three benzene rings with respect to the parallel subphthalocyanines. Thus, hexapropyl- (**2a,b**) and hexathiopentyl-substituted (**2c,d**) compounds display Q-bands at 501 and 559 nm,[17] respectively, that are blue-shifted by 70[14a] and 43 nm[10] relative to similarly substituted SubPcs. Changes in the axial substitution pattern produce little to negligible effects in the electronic spectra of the macrocycles owing to the presence of nodes at the boron atoms both in the HOMO and LUMO orbitals of boron(III) subporphyrazines.[15–17] In contrast, peripheral substitution produces striking effects in the electronic properties of these compounds. Hence, the red color of the thioalkyl-substituted SubPzs **2c,d** is intimately connected to their UV/Vis spectra and arises from a strong (the most intense of the spectrum), broad band at 444 nm assigned to $n \rightarrow \pi^*$ transitions from the peripheral sulfur lone-pair electrons into a π^* macrocyclic orbital, its high intensity being diagnostic of the strong π donation.[18,19] Equivalent charge-transfer bands are also observed in the electronic spectra of thioalkyl-substituted SubPcs, but in the latter case their relative intensity is one-third that of the corresponding Q-bands. This difference argues for a more effective electronic communication between the six thiolene groups and the macrocyclic core in boron(III) subporphyrazines related to SubPcs.[17] The enhanced interaction with the peripheral substituents within the SubPz class is also supported by the bathochromic shift produced in the Q-band upon peripheral thioalkyl substitution, which is twofold that produced in SubPcs.

Next, the macrocycles were tested in a series of radiolytic and photophysical experiments to explore their reduced, oxidized, and excited-state features.[20] Pulse radiolysis oxidation experiments were performed in oxygenated dichloromethane solutions, which are known to generate a series of oxidizing radicals. In particular, under aerated conditions solvent ionization and subsequent reaction with molecular oxygen is followed by the formation of peroxyl radicals, namely $^{\bullet}OOCH_2Cl$ or $^{\bullet}OOCHCl_2$. These radicals have been successfully employed to oxidize a wide variety of different tetrapyrrolic macrocyles (i.e., porphyrins, phthalocyanines, porphycenes, corrphycenes, etc.). Indeed, upon radical-induced oxidation of **2a** (5.0×10^{-6} M), for example, the kinetic traces showed an accelerated decay of the $^{\bullet}OOCH_2Cl$ or $^{\bullet}OOCHCl_2$ radicals that transformed into a residual absorption. Figure 3 shows typical differential absorption changes that were recorded at the conclusion of

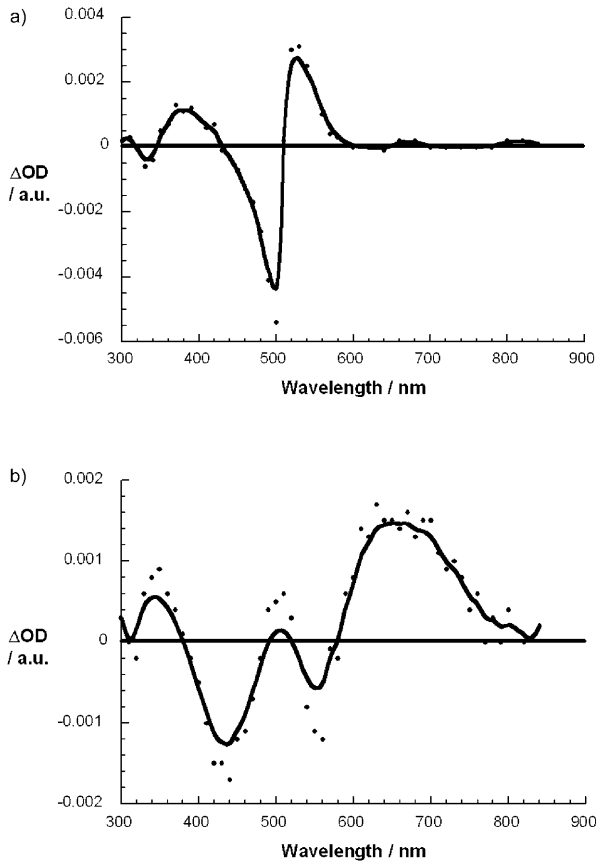

Figure 3. Differential absorption changes following pulse radiolytic oxidation of a) **2a** and b) **2c** in oxygenated dichloromethane with $^{\bullet}OOCH_2Cl$ or $^{\bullet}OOCHCl_2$ radicals.

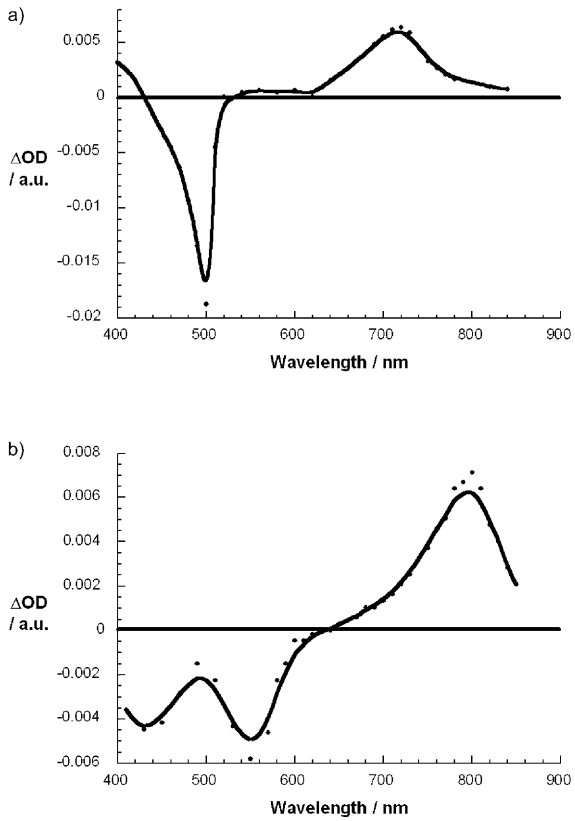

Figure 4. Differential absorption changes following pulse radiolytic reduction of a) **2a** and b) **2c** in a deoxygenated solvent mixture containing toluene, 2-propanol, and acetone with $(CH_3)_2{}^{\bullet}COH$ and $(CH_3)_2{}^{\bullet}CO^-$ radicals.

the $^{\bullet}OOCH_2Cl$- or $^{\bullet}OOCHCl_2$-induced oxidation of **2a** with a minimum at 500 nm that is flanked by maxima at 380 and 530 nm. Upon increasing the concentration of **2a** (i.e., up to 2.0×10^{-5} M), an accelerated formation of the one-electron radical cation and decay of the absorption by $^{\bullet}OOCH_2Cl$ and/or $^{\bullet}OOCHCl_2$ were found (Figure 3). The spectral features for the thioether-substituted subporphyrazine **2c** are, however, different: in agreement with the absorption spectra, we note two minima at 435 and 560 nm and the appearance of a maximum in the red region at 660 nm (Figure 3). On the time scale of the pulse radiolytic experiments (up to 400 μs), no notable decay of the one-electron oxidized **2a–d** species was registered. Thus, they are stable one-electron-reducing agents in, for example, the excited state.

To achieve reductive conditions required the use of a solvent mixture containing toluene, 2-propanol, and acetone (8:1:1), where in the absence of molecular oxygen strongly reducing $(CH_3)_2{}^{\bullet}COH$ and $(CH_3)_2{}^{\bullet}CO^-$ radicals are formed that are sufficiently reactive to reduce aromatic electron acceptors. The differential absorption spectrum commencing with the radiolytic reduction of **2a** is shown in Figure 4. Sets of minima at 500 nm and maxima at 720 nm are clearly discernable that are formed under pseudo-first-order conditions, leading us to postulate the one-electron reduction of **2a**. An increase or decrease in concentration led to the accelerated or decelerated formation, respectively, of the absorption of the radical anion. Similarly, the transient features associated with the $(CH_3)_2{}^{\bullet}COH$ and $(CH_3)_2{}^{\bullet}CO^-$ radicals were affected by the concentration of **2a**. Particularly relevant is the feature at 720 nm, as a diagnostic for the one-electron reduction of **2a**. Compound **2b** gives rise to the same maximum. Again, changes in the ground-state absorption spectrum, as they dominate the differences between **2a**,**b** and **2c**,**d**, are also reflected in the spectrum of the one-electron-reduced radical anions. Most important is the position of the diagnostic peak of the radical anion which is shifted for the latter (**2c**,**d**) to 800 nm. Up to 400 μs, the radical anions reveal no instability that might evolve from dimerization or protonation, for example.

Thus, **2a**–**d** are susceptible to one-electron-reduction and -oxidation reactions that lead, in turn, to stable reduced and oxidized species.[21] Notable are spectral characteristics that depend on the functionalization pattern of the SubPzs core and the redox state. This encouraged us to turn to excited-state features.

Next, we studied the fluorescence features as a complement to the ground-state absorption. Visible-light excitation in the 400–500 nm range (i.e., to photoexcite **2a** or **2b**) or in the 400–600 nm range (i.e., to photoexcite **2c** or **2d**) generates fluorescence patterns that are virtual mirror images to the absorption (Figure 5). In particular, maxima evolve at 520 nm (i.e., **2a** and **2b**) and 580 nm (i.e., **2c** and **2d**). Notably there are

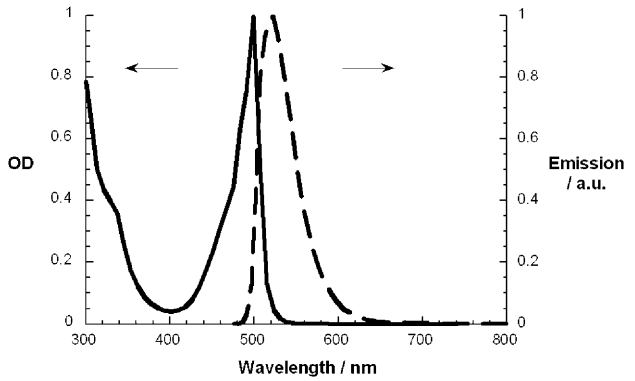

Figure 5. Absorption spectrum of **2a** in chloroform (solid line) and steady-state fluorescence spectrum of **2a** in toluene solutions (dashed line; excitation wavelength: 450 nm). Concentrations $\approx 10^{-5}$ M.

differences in the quantum yields. Thus, while **2a** and **2b** show high quantum yields (about 0.1) in the same range as similarly substituted SubPcs[2a] and in line with many tetrapyrrolic macrocycles, the specific functionalization in **2c** and **2d** evokes much weaker emissions. The quantum yields for the latter are only 0.002, which represents one-hundredth of that exhibited by the corresponding thioether-substituted subphthalocyanine.[2a] The fluorescence lifetimes at 520 and 580 nm display a similar trend. While **2a** and **2b** give rise to fairly long lifetimes of 1.25 ns $\pm$ 0.05 ns, the fluorescing states of **2c** and **2d** decay much faster with underlying lifetimes of 0.2 ns.

In the final part of our investigations, transient absorption spectroscopy (i.e., 150-fs laser pulses at 530 or 650 nm, and 8-ns laser pulses at 355 or 532 nm) was employed to probe the excited-state features. Monitoring the time evolution of the characteristic excited-state features is a convenient method to identify spectral features of the resulting photoproducts and to determine absolute rate constants for the intramolecular decays.

The differential spectra recorded immediately after the laser pulse for **2a** and **2b** are characterized by bleaching of the visible absorption at around 520 and broad absorption between 600 and 900 nm that has a maximum at 690 nm. These spectral attributes are indicative of the singlet excited state (E_S = 2.4 eV) and are formed with a rate constant of 1×10^{12} s^{-1}. The singlet excited-state features decay slowly (8.0×10^{8} s^{-1}) to the energetically lower-lying triplet excited state (E_T = 2.0 eV) predominantly by intersystem crossing. Characteristics of the triplet excited state include a slightly blue-shifted maximum that is centered around 660 nm, while the minimum remains unchanged at 500 nm. Figure 6 gives the differential absorption changes for **2a** in toluene.

Upon photoexcitation of **2c** and **2d**, population of the singlet excited state leads to differential absorption changes that include a broad transient bleaching between 450 and 590 nm with minima at 460 and 550 nm. Figure 7 shows how photoexcitation gives rise to a transient maximum in the red at 670 nm (i.e., singlet–singlet transition). Nevertheless, the metastable and fast decaying singlet–singlet features of **2c** and **2d**

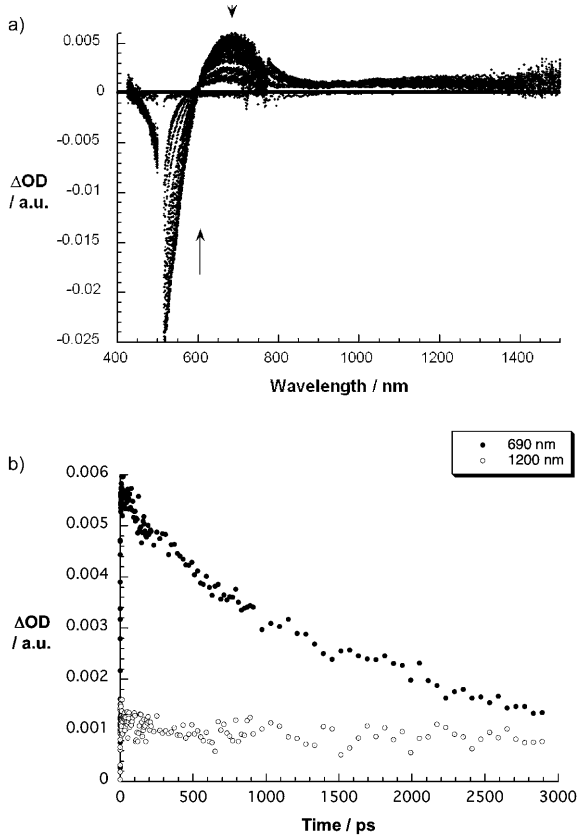

Figure 6. a) Differential absorption spectra (visible and near-infrared) obtained upon femtosecond flash photolysis (500 nm, 200 nJ) of **2a** in argon-saturated toluene with several time delays between 0 and 3000 ps at room temperature, illustrating the intersystem crossing. b) Time–absorption profiles at 690 and 1200 nm.

also give rise to an intersystem crossing process that is, however, markedly accelerated. Of importance here is the very short singlet lifetime (τ_S) of 200 ps $\pm$ 20 ps (5×10^{9} s^{-1}). This value is in accordance with our fluorescence lifetime measurements, where resolvable fluorescence decays were noted close to the time resolution of our instrumental setup. The accordingly formed triplets of **2c** and **2d** display in the visible region—like **2a** and **2b**—nearly unchanged minima at 460 and 550 nm and blue-shifted maxima at 630 nm. In addition, the triplet features reveal a transient maximum at 1300 nm.

In the complementary recorded nanosecond spectra, we see only the long-lived triplet–triplet transitions for **2a–d** with spectral changes that are in perfect agreement with those noted at the conclusion of the femto-/picosecond experiments. Under anaerobic conditions, the triplet lifetimes (τ_T) are 25 μs. All triplet excited states turned out to be quite oxygen-sensitive and are quenched with nearly diffusion-controlled kinetics to afford the formation of singlet oxygen.

Conclusions

We have demonstrated that the boron(III) subporphyrazine macrocycle can behave as an oxidizing or a reducing chromophore, giving rise to stable radical anion or radical cation spe-

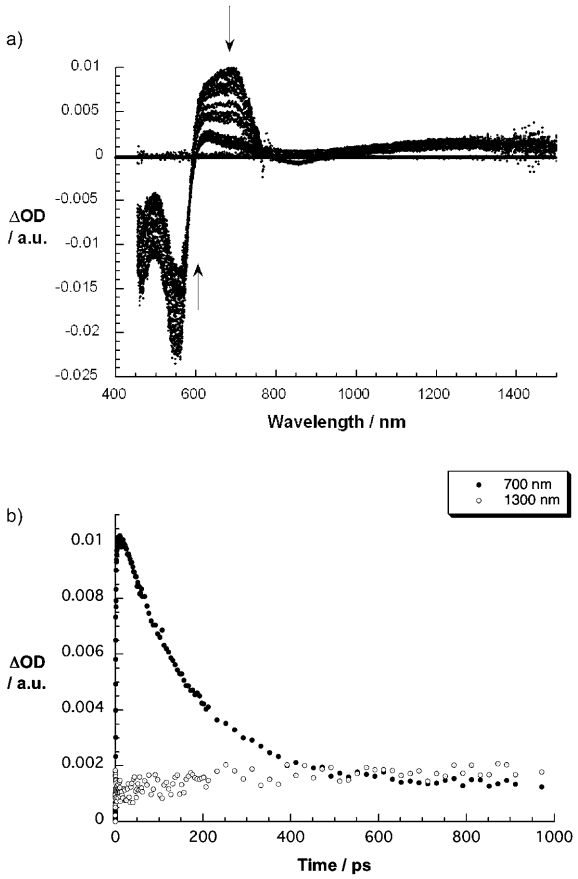

Figure 7. a) Differential absorption spectra (visible and near-infrared) obtained upon femtosecond flash photolysis (500 nm, 200 nJ) of **2c** in argon-saturated toluene with several time delays between 0 and 3000 ps at room temperature, illustrating the intersystem crossing. b) Time–absorption profiles at 700 and 1300 nm.

cies. All compounds are luminescent, exhibiting fluorescence quantum yields that are in the range known for SubPcs. Nevertheless, the peripheral substitution has a dramatic effect on the luminescence properties. Peripheral functionalization with, for example, thioethers imposes marginal fluorescence quantum yields and lifetimes compared to those for alkyl-substituted SubPzs and standard SubPc. Moreover, as with SubPcs, deactivation of the singlet excited state through intersystem crossing affords long-lived triplet excited states, amenable of being used as singlet-oxygen generators. Dye-sensitized generation of singlet oxygen provides a versatile reagent that plays a key role in oxidation reactions, including cycloaddition and ene reactions, to produce endoperoxides and hydroperoxides, respectively.[22] We strongly believe that SubPzs will emerge as an interesting class of chromophores employable in such photosensitization processes. Subporphyrazines are also promising electro- and photoactive materials for molecular photovoltaics.

Experimental Section

Photophysics: Femtosecond transient absorption studies were performed with 530 and 650 nm laser pulses (1 kHz, 150-fs pulse width) from an amplified Ti:Sapphire laser system (Model CPA 2101, Clark-MXR Inc.). Nanosecond laser flash photolysis experiments were performed with 355 or 532 nm laser pulses from a Quanta-Ray CDR Nd:YAG system (6-ns pulse width) in a front-face excitation geometry. Fluorescence lifetimes were measured with a Laser Strope Fluorescence Lifetime Spectrometer (Photon Technology International) with 337 nm laser pulses from a nitrogen laser fiber-coupled to a lens-based T-formal sample compartment equipped with a stroboscopic detector. Details of the Laser Strobe systems are described on the manufacturer's web site. Emission spectra were recorded with a SLM 8100 spectrofluorometer. The experiments were performed at room temperature. Each spectrum represents an average of at least five individual scans, and appropriate corrections were applied whenever necessary.

Pulse Radiolysis: Pulse radiolysis experiments were performed using 50 ns pulses of 15 MeV electrons from a linear electron accelerator (LINAC). Dosimetry was based on the oxidation of SCN^- to $(SCN)_2^{\bullet -}$, which in aqueous, N_2O-saturated solution takes place with $G \approx 6$ (G denotes the number of species per 100 eV, or the approximate μM concentration per 10 J absorbed energy). The radical concentration generated per pulse was varied between 1×10^{-6} M and 3×10^{-6} M.

Acknowledgements

The SFB 583, DFG (GU 517/4-1), FCI, the Office of Basic Energy Sciences of the U.S. Department of Energy, and COST (D-35/0015/05) are acknowledged for financial support. Grants from the Ministerio de Ciencia y Tecnología (CTQ2008–00418/BQU, Consolider-Ingenio 2010 CSD2007-00010 Nanociencia Molecular, ESF-MEC MAT2006-28180-E, SOHYDS), and Comunidad de Madrid MADRI-SOLAR ,S-0505/PPQ/0225) are gratefully acknowledged. M.S.R.-M. thanks also the Spanish MEC for a Ramón y Cajal contract.

Keywords: boron · photophysics · phthalocyanines · subporphyrazines

[1] a) G. de La Torre, C. G. Claessens, T. Torres, *Chem. Commun.* **2007**, 2000–2015; b) J.-J. Cid, J.-H. Yum, S.-R. Jang, M. K. Nazeeruddin, E. Martínez-Ferrero, E. Palomares, J. Ko, M. Grätzel, T. Torres, *Angew. Chem.* **2007**, *119*, 8510–8514; *Angew. Chem. Int. Ed.* **2007**, *46*, 8358–8362; c) B. C. O'Regan, I. Lopez-Duarte, M. V. Martínez-Díaz, A Forneli, J. Albero, A. Morandeira, E. Palomares, T. Torres, J. R. Durrant, *J. Am. Chem. Soc.* **2008**, *130*, 2906–2907, and references therein.

[2] a) C. G. Claessens, D. González-Rodríguez, T. Torres, *Chem. Rev.* **2002**, *102*, 835–853; b) T. Torres, *Angew. Chem.* **2006**, *118*, 2900–2903; *Angew. Chem. Int. Ed.* **2006**, *45*, 2834–2837.

[3] a) "Synthesis and Spectroscopic Properties of Phthalocyanine Analogs": N. Kobayashi in *The Porphyrin Handbook, Vol. 15, 100*, (Eds.: K. M. Kadish, K. M. Smith, R. Guilard), Academic Press, San Diego, CA, **2003**, pp. 161–262; b) P. Brothers, *Chem. Commun.* **2008**, 2090–2102; c) Y. Rio, M. S. Rodríguez-Morgade, T. Torres, *Org. Biomol. Chem.* **2008**, *6*, 1877–1894.

[4] a) A. Sastre, T. Torres, M. A. Díaz-García, F. Agulló-López, C. Dhenaut, S. Brasselet, I. Ledoux, J. Zyss, *J. Am. Chem. Soc.* **1996**, *118*, 2746–2747; b) C. G. Claessens, D. Gonzalez-Rodriguez, T. Torres, G. Martin, F. Agulló-Lopez, I. Ledoux, J. Zyss, V. R. Ferro, J. M. García de La Vega, *J. Phys. Chem. B* **2005**, *109*, 3800–3806, and references therein.

[5] a) N. Kobayashi, *J. Chem. Soc. Chem. Commun.* **1991**, 1203–1205; b) R. A. Kipp, J. A. Simon, M. Beggs, H. E. Ensley, R. H. Schmehl, *J. Phys. Chem. A* **1998**, *102*, 5659–5664.

[6] a) D. González-Rodríguez, T. Torres, M. A. Herranz, J. Rivera, L. Echegoyen, D. M. Guldi, *J. Am. Chem. Soc.* **2004**, *126*, 6301–6313; b) D. González-Rodríguez, T. Torres, M. M. Olmstead, J. Rivera, M. A. Herranz, L. Eche-

goyen, C. Atienza Castellanos, D. M. Guldi, *J. Am. Chem. Soc.* **2006**, *128*, 10680–10681; c) M. E. El-Khouly, S. H. Shim, Y. Araki, O. Ito, K-Y. Kay, *J. Phys. Chem. B* **2008**, *112*, 3910–3917.

[7] a) K. L. Mutolo, E. I. Mayo, B. P. Rand, P. Barry, S. R. Forrest, M. E. Thompson, *J. Am. Chem. Soc.* **2006**, *128*, 8108–8109; b) H. Gommans, D. Cheyns, T. Aernouts, C. Girotto, J. Poortmans, P. Heremans, *Adv. Funct. Mater.* **2007**, *17*, 2653–2658.

[8] a) C. G. Claessens, T. Torres, *Angew. Chem.* **2002**, *114*, 2673–2677; *Angew. Chem. Int. Ed.* **2002**, *41*, 2561–2565; b) T. Fukuda, J. R. Stork, R. J. Potucek, M. M. Olmstead, B. C. Noll, N. Kobayashi, W. S. Durfee, *Angew. Chem.* **2002**, *114*, 2677–2680; *Angew. Chem. Int. Ed.* **2002**, *41*, 2565–2568.

[9] C. G. Claessens, T. Torres, *J. Am. Chem. Soc.* **2002**, *124*, 14522–14523.

[10] S. H. Kang, Y.-S. Kang, W.-C. Zin, G. Olbrechts, K. Wostyn, K. Clays, A. Persoons, K. Kim, *Chem. Commun.* **1999**, 1661–1662.

[11] E. Palomares, M. V. Martínez-Díaz, T. Torres, E. Coronado, *Adv. Funct. Mater.* **2006**, *16*, 1166–1170.

[12] a) Y. Inokuma, J. H. Kwon, T. K. Ahn, M.-C. Yoon, D. Kim, A. Osuka, *Angew. Chem.* **2006**, *118*, 975–978; *Angew. Chem. Int. Ed.* **2006**, *45*, 961–964; b) N. Kobayashi, Y. Takeuchi, A. Matsuda, *Angew. Chem.* **2007**, *119*, 772–774; *Angew. Chem. Int. Ed.* **2007**, *46*, 758–760; c) Y. Inokuma, Z. S. Yoon, D. Kim, A. Osuka, *J. Am. Chem. Soc.* **2007**, *129*, 4747–4761; d) R. Mysliborski, L. Latos-Grazynski, L. Szterenberg, T. Lis, *Angew. Chem.* **2006**, *118*, 3752–3756; *Angew. Chem. Int. Ed.* **2006**, *45*, 3670–3674; e) Y. Inokuma, S. Y. Easwaramoorthi, S. Zi, D. Kim, A. Osuka, *J. Am. Chem. Soc.* **2008**, *130*, 12234–12235; f) Y. Inokuma, S. Easwaramoorthi, S. Y. Jang, K. S. Kim, D. Kim, A. Osuka, *Angew. Chem.* **2008**, *120*, 4918–4921; *Angew. Chem. Int. Ed.* **2008**, *47*, 4840–4843.

[13] a) Y. Inokuma, A. Osuka, *Dalton Trans.* **2008**, 2517–2526; b) E. A. Makarova, S. Shimizu, A. Matsuda, E. A. Luk'yanets, N. Kobayashi, *Chem. Commun.* **2008**, 2109–2111; c) P. Campomanes, M. I. Menendez, T. L. Sordo, *J. Porphyrins Phthalocyanines* **2007**, *11*, 815–821; d) T. Xu, R. Lu, X. Liu, P. Chen, X. Qiu, Y. Zhao, *Eur. J. Org. Chem.* **2008**, 1065–1071; e) E. Tsurumaki, S. Saito, K. S. Kim, J. M. Lim, Y. Inokuma, D. Kim, A. Osuka, *J. Am. Chem. Soc.* **2008**, *130*, 438–439.

[14] a) M. Geyer, F. Plenzig, J. Rauschnabel, M. Hanack, B. del Rey, A. Sastre, T. Torres, *Synthesis* **1996**, 1139–1151; b) N. Kobayashi, T. Ishizaki, K. Ishii, H. Konami, *J. Am. Chem. Soc.* **1999**, *121*, 9096; c) R. Potz, M. Göldner, H. Hückstädt, U. Cornelissen, A. Tutass, H. Homborg, *Z. Anorg. Allg. Chem.* **2000**, *626*, 588–596.

[15] a) A. K. Eckert, M. S. Rodríguez-Morgade, T. Torres, *Chem. Commun.* **2007**, 4104–4106.

[16] M. S. Rodríguez-Morgade, C. G. Claessens, A. Medina, D. González-Rodríguez, E. Gutiérrez-Puebla, A. Monge, I. Alkorta, J. Elguero, T. Torres, *Chem. Eur. J.* **2008**, 1342–1350.

[17] a) M. S. Rodríguez-Morgade, S. Esperanza, T. Torres, J. Barberá, *Chem. Eur. J.* **2005**, *11*, 354–360; b) J. R. Stork, J. J. Brewer, T. Fukuda, J. P. Fitzgerald, G. T. Yee, A. Y. Nazarenko, N. Kobayashi, W. S. Durfee, *Inorg. Chem.* **2006**, *45*, 6148–6151.

[18] For a comprehensive review on porphyrazines, see: M. S. Rodríguez-Morgade, P. V. Stuzhin, *J. Porphyrins Phthalocyanines* **2004**, *8*, 1129–1166.

[19] D. P. Goldberg, A. Garrido Montalban, A. J. P. White, D. J. Williams, A. G. M. Barrett, B. M. Hoffman, *Inorg. Chem.* **1998**, *37*, 2873–2879.

[20] a) D. M. Guldi, H. Hungerbühler, K.-D. Asmus, *J. Phys. Chem. A* **1997**, *101*, 1783–1786; b) D. M. Guldi, *J. Phys. Chem. A* **1997**, *101*, 3895–3900.

[21] Complementary electrochemical experiments in acetonitrile/toluene (4:1 v/v), a glassy carbon working electrode, a Pt counter electrode, and a Ag wire reference electrode revealed reduction and oxidation potentials for **2a** at -1.74 V and $+0.82$ V versus Fc/Fc^+, respectively. The corresponding potentials for **2c** were -1.17 V and $+1.03$ V versus Fc/Fc^+. For comparison with related macrocycles, see: N. Rubio, A. Jiménez-Banzo, T. Torres, S. Nonell, *J. Photochem. Photobiol. A* **2007**, *185*, 214–219.

[22] M. J. Fuchter, B. M. Hoffman, A. G. M. Barrett, *J. Org. Chem.* **2006**, *71*, 724–729.

Received: September 16, 2008
Published online on December 29, 2008

